Northumbria Research Link

Northumbria
University
NEWCASTLE

Research Article | Vol. 28, No. 12 / 8 June 2020 / Optics Express 18241
Optics EXPRESS

Experimental multi-user VLC system using non-orthogonal multi-band CAP modulation

P. PEŠEK,[1,*] P. A. HAIGH,[2] O. I. YOUNUS,[3] P. CHVOJKA,[1] Z. GHASSEMLOOY,[3] AND S. ZVÁNOVEC[1]

[1] *Wireless and Fibre Optics Group, Department of Electromagnetic Field, Faculty of Electrical Engineering, Czech Technical University in Prague, Prague 16627, Czech Republic*
[2] *Intelligent Sensing and Communications Group, Newcastle University, NE1 7RU, UK*
[3] *Optical Communications Research Group, Faculty of Engineering and Environment, Northumbria University, NE1 8ST, UK*
[*] *pesekpe3@fel.cvut.cz*

Abstract: This paper provides experimental results for a multi-user visible light communications system using multi-band carrier-less amplitude and phase (*m*-CAP) modulation scheme. We optimize the system performance by adapting pulse shaping filter parameters, subcarrier spacing and allocating different baud rates to individual sub-bands called allocated *m*-CAP (A*m*-CAP). We show that a maximal system data rate of ~468 Mb/s for four users can be supported while gaining higher flexibility for optimization and the same or lower computational complexity compared with the conventional *m*-CAP scheme.

1. Introduction

In recent years, visible light communication (VLC) has received a growing interest within both industrial and academic communities as a complementary technology to the radio frequency wireless systems in 5G and beyond networks [1]. In VLC systems, high-brightness light emitted diode (LED)-based lights are used to provide illumination, indoor localization and data communications in indoor environment at the moment – outdoor-based systems are also being considered [2]. The vast majority of current research activities have focused on the data rate R_b improvement i.e., from hundreds of Mb/s to a few Gb/s over the short line of sight transmission ranges (from few centimeters to few meters) [3,4]. Two of the most popular options, which have been widely adopted and reported in the literature to improve R_b, are the spectrally efficient quadrature amplitude modulation (QAM) symbol-based multicarrier modulation schemes including orthogonal frequency division multiplexing (OFDM) and carrier-less amplitude and phase (CAP) modulation [5–8]. However, the OFDM-based VLC systems with high peak-to-average power ratio (PAPR) are highly sensitive to the nonlinearity of the amplifiers, LEDs (i.e., power-current characteristics), which leads to the system performance deterioration [9].

An alternative to OFDM is the CAP modulation scheme, which has been investigated in intensity modulation and direct detection (IM-DD) VLC systems offering relatively higher R_b compared with OFDM using electrical components of limited bandwidth and lower complexity. In [9], OFDM- and CAP-based VLC links using a single red, green and blue (RGB) LEDs were experimentally investigated showing CAP offering 19% higher R_b compared with OFDM over the same link span [10]. An experimental *m*-CAP VLC link over a 1 m distance with a high spectral efficiency of 4.85 b/s/Hz for a single user scheme was demonstrated in [11]. Further modification of subcarrier spacing below orthogonality can improve the spectral efficiency about 25% for a direct LOS link without considering a multi-user scenario, which was demonstrated in [12]. In [13], an additional 20% improvement in the data rate was achieved by increasing the baud rates of individual non-orthogonal sub-bands while utilising the same signal bandwidth. This technique

#393813 https://doi.org/10.1364/OE.393813
Journal © 2020 Received 27 Mar 2020; revised 9 May 2020; accepted 26 May 2020; published 3 Jun 2020

Optics EXPRESS

is known as an expanded non-orthogonal super-Nyquist *m*-CAP (*m*-ESCAP). Another alternative approach is based on splitting the signal into unequally spaced subcarriers, which is known as variable *m*-CAP (V*m*-CAP) that offers a ~30% improvement in R_b for a bandlimited VLC link with 6 subcarriers compared with the conventional 6-CAP and also reduced computational complexity [14]. However, increasing the number of bands will lead to a higher number of pulse shaping finite impulse response (FIR) filters, i.e., 4 FIR filters per band, thus significantly higher computational complexity. The higher sub-band orders of *m*-CAP are vulnerable to timing errors. For instance, in [15] a detailed analysis of the timing jitter in 40 Gb/s fiber optics system was given. high-order CAP VLC link with an aggregate data rate of 8 Gb/s over a link span of 1 m using a hybrid post equalizer (i.e., a linear Volterra series and a decision-directed least mean squares equalizer) over four wavelengths was reported in [16]. In [17], the scheme for 5G mobile networks combining *m*-CAP and non-orthogonal multiple access (NOMA) was experimentally evaluated over the W-band millimeter wave radio-over fiber system.

Current research, however, has mostly focused on point-to-point single-user scenarios. In an effort to transform VLC into a multi-user, flexible technology, more experimental investigation of the multi-user frequency division multiple access (FDMA) scheme has to be done. Orthogonal FDMA (OFDMA) was adopted in the 4G wireless networks, where multiple access is achieved by assigning subsets of sub-carriers to different users, thus allowing simultaneous data transmission from several users [18]. In OFDMA, the transmit power is allocated to individual users based on the signal-to-noise ratio (SNR). A comparison of the bit error rate (BER) performance, receiver (Rx) complexity, and PAPR for two versions of OFDMA were reported in [19]. An interleave division multiple access OFDMA with asymmetrically clipped optical OFDM offers higher power efficiency than conventional OFDMA, especially at higher R_b. In order to increase the system throughput and improve the signal to interference plus noise ratio (SINR) of the users at the cell boundaries a multi-point joint transmission VLC network was proposed in [20]. This scheme achieved data throughput improvement of 68% compared with a static resource partitioning system. Alternatively, such frequency reuse could be utilised to improve the performance of the edge user. In [21], a combination of dc-biased optical OFDM and fractional frequency reuse in optical cell networks was reported, which significantly reduced the inter-channel interference (ICI) and offered a good balance between the average spectral efficiency and system complexity. Time division multiple access (TDMA) can achieve a fair user experience compared with FDMA as is discussed for example in [22], FDMA-based schemes (i.e., *m*-CAP, OFDM, etc.) offer a number of advantages including no need for highly accurate two-level synchronisation and compatibility with the radio frequency based wireless technology as in 4G and 5G [23,24].

The first experimental verification of the multi-user *m*-CAP with a wavelength division multiplexed VLC system using a single RGB LED for serving up to 9 users was reported in [24]. A multi-user scheme of 20-CAP with a total R_b of 162.5 Mb/s for up to 20 users was reported in [23], where optimization of transmit filters' parameters was investigated.

Nevertheless, to the best of authors' knowledge, no works, on the experimental investigation of allocating different bandwidth of the individual subcarriers to users, called allocated *m*-CAP (A*m*-CAP), for multi-user scenarios have been reported yet. The primary objective of this paper is to investigate the performance of an optimized A*m*-CAP system with the same allocated data rate per user. To validate this, we have developed an experimental test-bed for both the conventional *m*-CAP and A*m*-CAP as a multi-user system by optimizing: *(i)* the subcarrier spacing, where the subcarrier bandwidth is purposely compressed below orthogonality by means of squeezing carrier frequencies; *(ii)* the roll-off factor, which can support higher spectral usage based on controlling the excess bandwidth of individual subcarriers; and *(iii)* a combination of carrier spacing and the roll-off factor to achieve the maximal spectrum efficiency and almost the same data throughputs for the users in a multi-user system. We show that, A*m*-CAP offers improved allocation flexibility (i.e., the same data throughput for all four users in this case) or lower computational complexity

Optics EXPRESS

compared with conventional m-CAP. Furthermore, we show that, following optimization the spectral efficiency can be improved by about 12% to 4.68 b/s/Hz.

2. System setup

The schematic block diagram of the proposed multi-user VLC system is depicted in Fig. 1. A pseudorandom binary sequence of length 2^{15}-1 is generated for each subcarrier and mapped into complex symbols of M-QAM, where M is the order of modulation. Note, the data stream per user is allocated into one or more sub-bands depending on the number of users per cell and a number of m-CAP bands. The mapped data is up-sampled by means of zero-padding (i.e., the number of zeros/symbol is based on [11]):

$$n_s = 2 \cdot \lceil 2m(1+\beta) \rceil \tag{1}$$

where β is roll-factor of the transmit/receiver filters and $\lceil \cdot \rceil$ is the ceiling function. Then data is split into its real and imaginary components (i.e., in-phase (I) and quadrature (Q)) prior to being applied to the square root raised cosine (SRRC) pulse shaping filter pairs $f_I^n(t)$ and $f_Q^n(t)$, respectively. Note, filters impulse responses form a Hilbert pair, i.e., being orthogonal in the time domain and shifted by 90° in phase. The impulse responses are given as the product of the SRRC filter impulse response and the sine and cosine wave, as follow [25]:

$$f_I^n(t) = \left[\frac{sin[\gamma(1-\beta)] + 4\beta \frac{t}{T_s} cos[\gamma\delta]}{\gamma[1-(4\beta\frac{t}{T_s})^2]} \right] cos(2\pi f_c^n t) \tag{2}$$

$$f_Q^n(t) = \left[\frac{sin[\gamma(1-\beta)] + 4\beta \frac{t}{T_s} cos[\gamma\delta]}{\gamma[1-(4\beta\frac{t}{T_s})^2]} \right] sin(2\pi f_c^n t) \tag{3}$$

where T_s is the symbol duration, n denotes the index of a subcarrier, $\gamma = \pi t/T_s$ and $\delta = 1+\beta$. The frequencies of subcarriers, generated by the pulse shaping transmit filters, are given by [13]:

$$f_c^n = B_{tot}(1+\alpha)\left(\frac{1}{2m} - \frac{(n-1)(1+\alpha m - m)}{m(m-1)} \right) \tag{4}$$

where B_{tot} is defined as total signal bandwidth and α is the bandwidth compression factor. In m-CAP, α is set to 0 in order to maintain subcarrier orthogonality. However, in m-ESCAP, the carrier frequencies are shifted to lower values. On the other hand, for Am-CAP, the frequencies of subcarriers are given by:

$$\begin{aligned} f_c^n &= \frac{R_{b-Max}\delta}{2k_n n(1+\alpha)} && \text{, for } n = 1 \\ f_c^n &= \frac{R_{b-Max}\delta}{n(1+\alpha)2k_n} + \sum_{i=1}^{n-1} \frac{R_{b-Max}\delta}{n(1+\alpha)k_i} && \text{, otherwise} \end{aligned} \tag{5}$$

where R_{b-Max} is the maximal system data rate for n users and k is a number of bits/symbol for QAM. The output of CAP-based transmitter (Tx) is given by [25]:

$$s(t) = \sqrt{2} \sum_{n=1}^{m} \left(s_I^n(t) * f_I^n(t) - s_Q^n(t) * f_Q^n(t) \right) \tag{6}$$

where $s_I^n(t)$ and $s_Q^n(t)$ are the I and Q M-QAM symbols, respectively for the n^{th} subcarrier and $*$ represents time-domain convolution. With an increasing number of sub-bands, the allocation

Optics EXPRESS

flexibility grows at the cost of significantly increased computational complexity. The complexity of the m-CAP can be expressed as [26]:

$$C_{m-CAP} = R_s \left(2m + 2\sum_{n=1}^{m} n_n L_s\right) \tag{7}$$

where n_n is required sample count per symbol for the n^{th} subband, L_s is filter symbol length and R_s is baud rate. For example, the complexity of m-CAP almost halves for m when changed from $m = 8$ to 4. This is mainly because m-CAP complexity is proportional to m^2, i.e., O(m^2) [26], as indicated by Eq. (7), which significantly handicaps the higher orders of m-CAP.

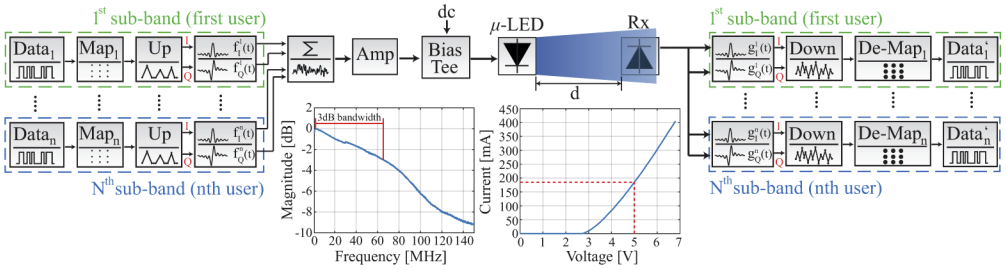

Fig. 1. The schematic block diagram of the experimental m-CAP VLC system. "Up", "Down", "Map" and "Amp" refer to up-sampling, down-sampling, mapper and amplifier, respectively. The left inset depicts measured LED frequency response with the highlighted 3 dB bandwidth of ~67 MHz. The right inset shows the measured I-V curve of the μ-LED.

The generated signal $s(t)$ in the Matlab is loaded into a signal generator (Teledyne LeCroy T3AWG3252), the output of which is amplified and dc-biased prior to IM of the LED. The light source used is a blue μ-LED with a wavelength of 449 nm, a linewidth of 14.6 nm and a measured 3 dB bandwidth of ~67 MHz, see the inset in Fig. 1. The signal is transmitted over a 20 cm free space channel, which is limited by the transmit power of the μ-LED. However, the transmission distance can be increased by using *(i)* high power μ-LEDs and *(ii)* array μ-LEDs as in attocells configurations [27,28]. At the Rx side, we use a combination of an optical lens

Table 1. VLC system parameters

Parameters	Value
Pseudorandom binary sequence	2^{15}-1
μ-LED bias current	185 mA
Total signal bandwidth	100 MHz
Rx biconvex lens focal length	25 mm
Signal generator peak-to-peak voltage	3.6 V
Amplification	2x
BER limit	3.8×10^{-3}
Filter length	16 symbols
Roll-off factor (No-optimization)	0.2
Roll-off factor (Carrier-optimization)	0.2
Rx wavelength range	200–1000 nm
Rx maximum responsivity	50 A/W at 600 nm
Rx bandwidth	400 MHz

Optics EXPRESS

with a focal length of 25 mm (not shown in Fig. 1) and optical Rx (APD430A2 Thorlabs with a low noise avalanche photo-detector and a trans-impedance amplifier) to regenerate the electrical CAP signal $s_r(t)$. Following capturing of $s_r(t)$ by a real-time oscilloscope (Keysight DSO9104A) and filtering by a low-pass filter (LPF) with 200 MHz bandwidth, the signal is resampled to the sampling frequency of the transmitted signal and applied to the time-reversed filter pairs at Rx, which are matched to the Tx filters, thus allowing each user to recover their data.

Following down-sampling and demodulation, the recovered M-QAM symbols allocated to the users are compared with the transmitted data for the BER estimation. In order to improve the system throughput, we have used a pilot binary phase-shift keying (BPSK) signal to load an appropriate k to individual subcarriers based on the measured SNR as in [29]. All the key system parameters adopted are listed in Tab. 1.

3. Experimental results

This section presents the results for R_b of optimized conventional m-CAP scheme and Am-CAP under the same transmission conditions. Here, we consider three optimization schemes: *(i)* uniform optimization of β, i.e., $0 \leq \beta \leq 1$, where higher values of β result in δ-times wider bandwidth; *(ii)* optimization of α, i.e., $0 \leq \alpha \leq 0.3$, using m-ESCAP, where the spacing between carriers is uniform and the total system bandwidth is limited to 100 MHz. Note, reducing the carrier spacing leads to inter-carriers interference (ICI), thus resulting in higher BER [12]; *(iii)* full-optimization, which is a combination of *(i)* and *(ii)*. The BER target is set to the 7% forward error correction (FEC) limit of 3.8×10^{-3}. The optimization process is depicted in Fig. 2. A full-optimization is realized in three steps. *(i)* Uniform optimization where the global values are set for all the subcarriers (i.e., m, α, β, f_c and M based on the loading algorithm). *(ii)* Splitting the algorithm into two branches, where the first and second branches are used for optimizing β and α with the step sizes of 0.05 and 0.01, respectively. Note, in full-optimisation we have used the β values from the β optimization to reduce brute force methods in one loop.

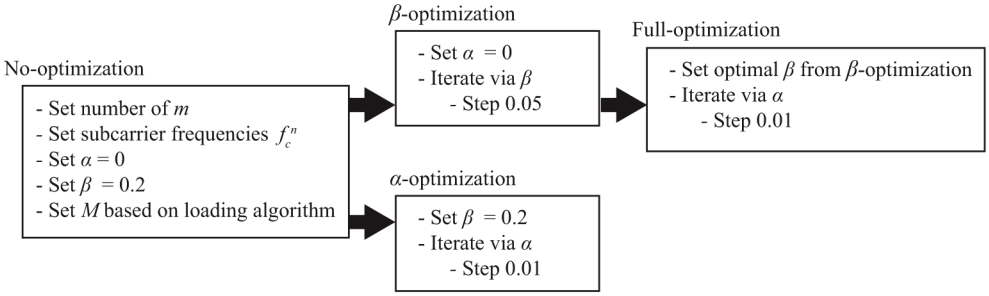

Fig. 2. Optimization process for obtaining system parameters of CAP-based scheme.

The bandwidth optimization of Am-CAP was based on the assumption the frequency response is flat. In that case, to achieve a maximum R_b, we used BPSK signal to load an appropriate number of bits/symbol to individual sub-bands based on the measured SNR. For instance, in 4-CAP the constellation size of the individual subcarriers is $M = \{64, 32, 32, 16\}$, however the same values can be expected even for A4-CAP due to flat frequency response. The carrier frequencies are then given by Eq. (5). Due to optimisation techniques, the calculated bandwidths are slightly changed, for example, calculated subcarriers bandwidth for A4-CAP are 20.8, 23, 23, 32.8 MHz, optimal subcarriers bandwidth are 20.4, 24.5, 24.5, 30.6 MHz. However, this first estimate significantly simplifies the ideal bandwidth allocation.

The concept of the proposed schemes is best illustrated using the frequency spectrum, see Fig. 3. The ideal spectra for conventional orthogonal m-CAP and Am-CAP are shown in Figs. 3(a)

Optics EXPRESS

and (b), respectively, for $m = 2$ and for $\beta = 0.1$. With α-optimisation subcarriers of m-ESCAP and Am-CAP overlap as depicted in Figs. 3(c) and (d), respectively. Note, m-ESCAP and conventional m-CAP have the same B_{tot} (i.e., 100 MHz), and with no changes in the subcarrier spacing (i.e., f_c remain the same). Note the followings: *(i)* to improve the data rate while maintaining the same B_{tot}, the individual sub-bands can be expanded by increasing R_s of the individual subcarriers; and *(ii)* compressing the sub-bands beyond their orthogonality limit will result in electrical power penalty due to sub-band overlapping and improved spectral efficiency with no additional computational complexity at the receiver but at the cost of higher BER [12]. Finally, Figs. 3(e) and (f) show the ideal spectra for non-orthogonal 4-CAP and A4-CAP for $\beta = \alpha = 0.1$. Note, A4-CAP offers one additional dimension for tuning of the system resources (i.e., allocation of different bandwidth to subcarriers and therefore higher/lower data rate per user as and when needed) with no increased computation complexity.

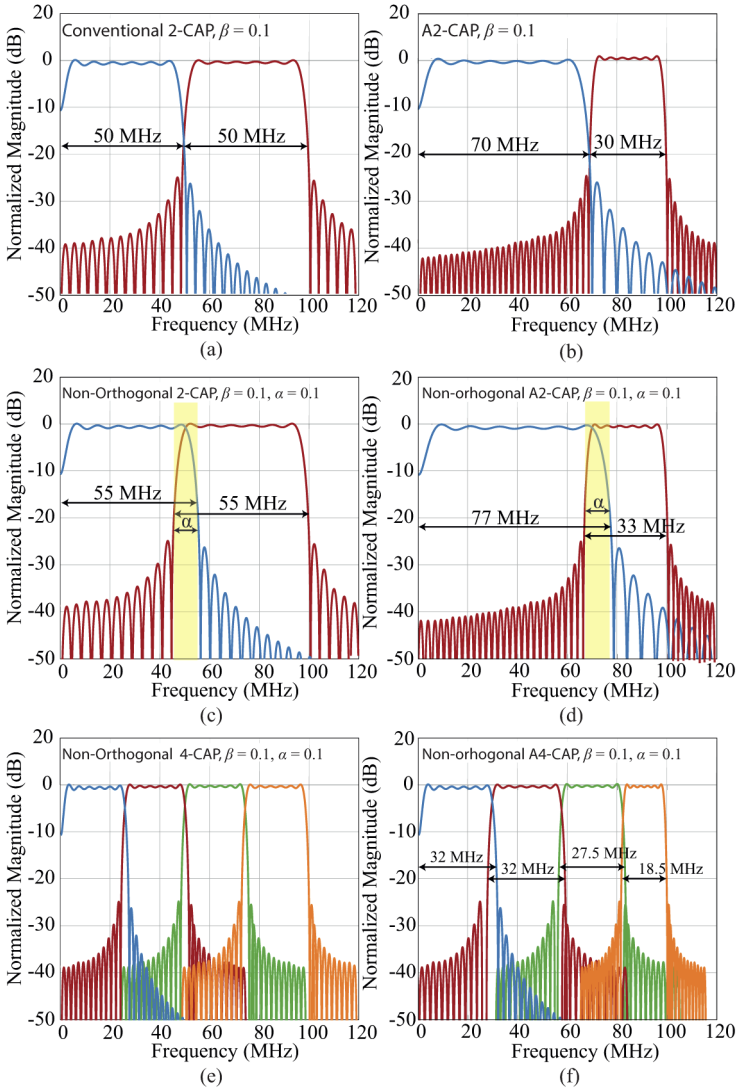

Fig. 3. Ideal spectra of (a) 2-CAP and (b) A2-CAP wtih $\beta = 0.1$, (c) 2-ESCAP and (d) the proposed multi-user A2-CAP with $\alpha = 0.1$ and $\beta = 0.1$. (e) and (f) show spectra of individual sub-carriers for 4-ESCAP and A4-CAP with the allocated bandwidths for users.

Optics EXPRESS

3.1. Conventional m-CAP

Figure 4(a) illustrates the maximum system data rate R_{b-Max} as a function of the m-CAP order with and without optimization. Note, with no optimization, β is set to 0.2, and R_{b-Max} of 416 Mb/s is achieved for 3- and 4-CAP and further increment of m does not improve the system performance in contrast to [11]. This is because of the μ-LED magnitude response decreases only ~6 dB over the 100 MHz frequency span, see the inset of Fig. 1, and the fact that higher sub-bands are more sensitive to the timing jitter and therefore synchronisation instability [15,30]. Higher-order CAP (i.e., $m > 4$) offers higher flexibility between the end-users at the cost of significantly increased system complexity and reduced R_{b-Max} (e.g., for 12-CAP R_{b-Max} is about 40 Mb/s lower compared with 4-CAP). For instance, in 10-CAP the constellation size of the individual subcarriers is $M = \{64, 64, 64, 32, 32, 16, 16, 16, 8, 8\}$. For 4-CAP with the carrier (β of 0.2 and α of 0.08), roll-off (β of 0.1) and full (β of 0.1 and α of 0.03), optimizations, R_{b-Max} are increased by 4, 9 and 13%, respectively, with respect to the 4-CAP without optimization. Note, for the highest data rate observed for 4-CAP with full-optimisation (i.e., β of 0.1 and α of 0.03) the maximum system spectral efficiency is 4.68 b/s/Hz.

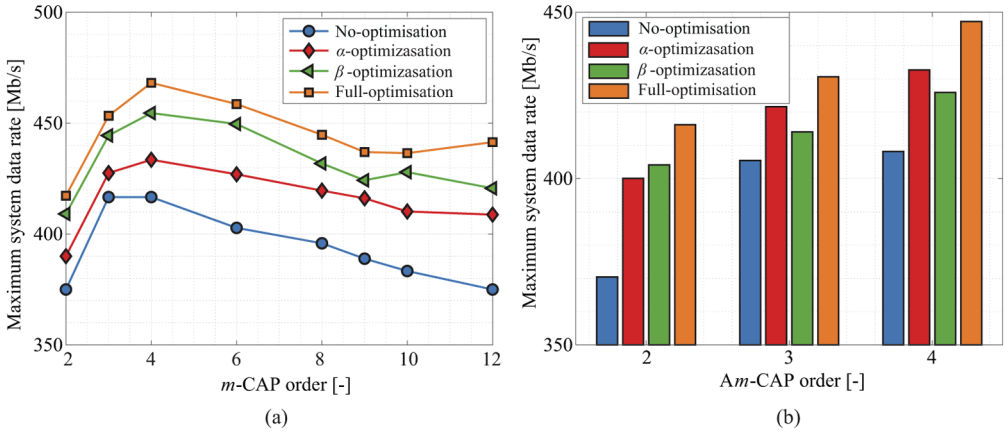

Fig. 4. Experimentally measured maximum data rate with and without optimization of (a) m-CAP and (b) Am-CAP

3.2. Am-CAP

Figure 4(b) shows the maximum system data rate R_{b-Max} as a function of m in Am-CAP shared between 2–4 users with and without optimisation. Am-CAP offers improved flexibility of multi-user allocation and M-ary assignment compared with the m-CAP scheme at the cost of increased PAPR [31]. For 2 users (i.e., A2-CAP), the system achieves R_{b-Max} of 370.42 Mb/s with the bandwidth allocations of 44.5 and 55.5 MHz and 32-QAM and 16-QAM, which increases to 400 and 404 Mb/s for the α- and β-optimisations, respectively. Note, Am-CAP with full-optimization (β and α of 0.1 and 0.03, respectively) offers 11% improvement in R_{b-Max}. The same patterns are observed for both A3- and A4-CAP. However, note, the α outperforms the β-optimization. This is due to the optimal β values of 0.175 and 0.15 for A3- and A4-CAP, respectively, which is close to the default value of 0.2 for no-optimisation. Note, R_{b-Max} of 447.21 Mb/s is achieved for A4-CAP with full-optimization.

3.3. Multi-user system

In a multi-user environment, the user's reception angle will considerably influence the system's BER performance. Figure 5(a) depicts the BER performance as a function of the user's orientation

Optics EXPRESS

(i.e., angle) respect to the Tx for a range of R_{b-Max} (full-optimisation for 4-CAP, reduction about 15% and 30%). The results show that, at the FEC limit, a maximum tolerance angle of 25° is accepted by the user with the highest R_{b-Max} of 468.18 Mb/s followed by R_{b-Max} of 401.81 and 327.73 Mb/s with the angles of 40° and 48°, respectively. Note, for R_{b-Max} of 327.73 Mb/s (i.e., 30% reduction) only ~7.5° of improvement is observed.

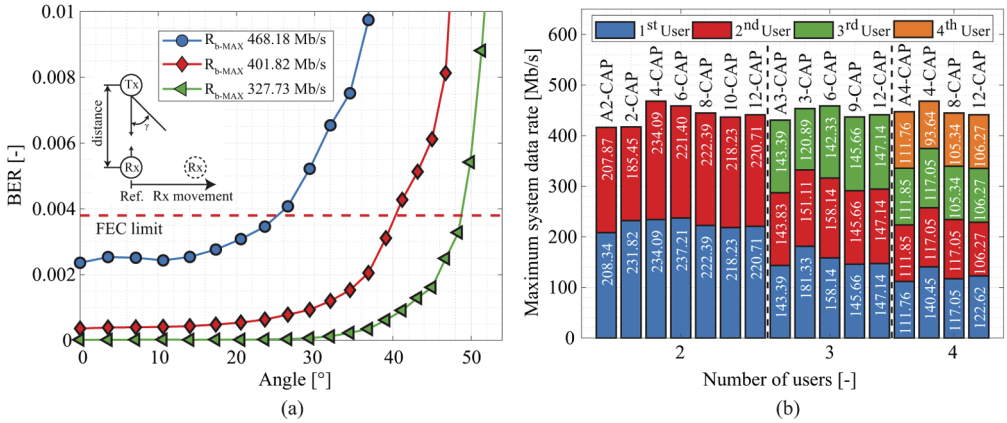

Fig. 5. Experimentally measured: (a) BER as a function of the angle user's with respect to the Tx for range of maximum data rates and (b) maximal data rate per user for *m*-CAP and A*m*-CAP schemes. The inset in (a) depicts the maximal acceptance angle.

Figure 5(b) shows the R_{b-Max} per users for the *m*-CAP and A*m*-CAP with full-optimization and 2–4 users. In the case of conventional *m*-CAP, more subcarriers can be allocated to the user, where subcarrier allocation is realized prior to transmission in the absence of uplink in this scenario. The main goal of subcarrier allocation is to ensure the same R_b between the users. In the case of 2 users, A2-CAP offers the same R_b of ~208 Mb/s per user compared with 231.82 and 185.45 Mb/s for the 1st and 2nd user, respectively, for 2-CAP with the same filter computational complexity. For higher *m*, the system elasticity significantly grows and slightly higher R_b can be supported at the cost of much higher filter computational complexity [26]. For 3 users, 9-CAP (with β of 0.1 and α of 0.03) is the first order, which provides the same data rate allocation. Note, the R_{b-Max} is only about 2 Mb/s per user higher than A3-CAP, but at the cost of an additional 24 FIR filters. For A4-CAP, the subcarrier bandwidths are 20.4, 24.5, 24.5, 30.6 MHz with the corresponding *M*-QAM sizes of 64, 32, 32, and 16 for the 1st, 2nd, 3rd and 4th user, respectively. In higher orders *m*-CAP each sub-band will need additional 4 FIR filters, which means increased computational complexity. However, A4-CAP offers roughly the same system date rate, higher allocation flexibility and significantly lower computational complexity compared with 8- and 12-CAP. For instance, in 12-CAP the constellation size of the individual subcarriers is $M = \{64, 64, 64, 32, 32, 32, 16, 16, 16, 8, 8, 8\}$. For 4 users, the variable scheme shows the best performance supporting similar allocated R_b.

4. Conclusion

In this paper, we demonstrated a maximum system data rate of 468.18 Mb/s by optimizing both α and β parameters. Such a system fulfils the 7% FEC limit up to a reception angle of 25°. By decreasing the the system's bit rate about ~30%, the reception angle is improved up to almost 50° (i.e., 100° full-angle) which significantly enhances the coverage of the VLC system. We designed and experimentally investigated an A*m*-CAP modulation technique for multiple users, which offers a similar data rate as the conventional *m*-CAP modulation scheme but significantly lower filter requirements. With the same computation complexity as conventional *m*-CAP, A*m*-CAP

Optics EXPRESS

offers higher allocation flexibility for four users scenario and therefore it is the suitable candidate for highly flexible data allocation scheme for indoor wireless communications.

Funding

Grant Agency of the CTU in Prague (SGS20/166/OHK3/3T/13); H2020 Marie Sklodowska-Curie Innovative Training Network (VisIoN 764461).

Acknowledgments

The authors would like to acknowledge the μ-LEDs material aid given by the Plessey Co. Ltd.

Disclosures

The authors declare no conflicts of interest.

References

1. Z. Ghassemlooy, L. N. Alves, S. Zvanovec, M. A. Khalighi, S. Zvánovec, and M. A. Khalighi, *Visible Light Communications: Theory and Applications* (CRC-Taylor & Francis Group, 2017).
2. Z. Ghassemlooy, S. Arnon, M. Uysal, Z. Xu, and J. Cheng, "Emerging Optical Wireless Communications-Advances and Challenges," IEEE J. Select. Areas Commun. **33**(9), 1738–1749 (2015).
3. S. Zvanovec, P. Chvojka, P. A. Haigh, and Z. Ghassemlooy, "Visible Light Communications Towards 5G," Radioeng. **24**(1), 1–9 (2015).
4. S. Kumar and P. Singh, "A Comprehensive Survey of Visible Light Communication: Potential and Challenges," Wirel. Pers. Commun. **109**(2), 1357–1375 (2019).
5. D. Tsonev, C. Hyunchae, S. Rajbhandari, J. J. D. McKendry, S. Videv, and E. Gu, "A 3-Gb/s Single-LED OFDM-Based Wireless VLC Link Using a Gallium Nitride μLED," IEEE Photon. Technol. Lett. **26**(7), 637–640 (2014).
6. J. Armstrong, "OFDM for Optical Communications," J. Lightwave Technol. **27**(3), 189–204 (2009).
7. X. Huang, Z. Wang, Y. W. J. Shi, N. Chi, J. Shi, Y. Wang, and N. Chi, "1.6 Gbit/s Phosphorescent White LED Based VLC Transmission Using a Cascaded Pre-Equalization Circuit and a Differential Outputs PIN Receiver," Opt. Express **23**(17), 22034–22042 (2015).
8. K. O. Akande, P. A. Haigh, and W. O. Popoola, "On the Implementation of Carrierless Amplitude and Phase Modulation in Visible Light Communication," IEEE Access **6**, 60532–60546 (2018).
9. R. Mesleh, H. Elgala, and H. Haas, "LED Nonlinearity Mitigation Techniques in Optical Wireless OFDM Communication Systems," J. Opt. Commun. Netw. **4**(11), 865–875 (2012).
10. F. M. Wu, C. T. Lin, C. C. Wei, C. W. Chen, Z. Y. Chen, H. T. Huang, and S. Chi, "Performance Comparison of OFDM Signal and CAP Signal over High Capacity RGB-LED-Based WDM Visible Light Communication," IEEE Photonics J. **5**(4), 7901507 (2013).
11. P. A. Haigh, A. Burton, K. Werfli, H. L. Minh, E. Bentley, P. Chvojka, W. O. Popoola, I. Papakonstantinou, and S. Zvanovec, "A Multi-CAP Visible-Light Communications System With 4.85-b/s/Hz Spectral Efficiency," IEEE J. Select. Areas Commun. **33**(9), 1771–1779 (2015).
12. P. A. Haigh, P. Chvojka, Z. Ghassemlooy, S. Zvanovec, and I. Darwazeh, "Visible Light Communications: Multi-Band Super-Nyquist CAP Modulation," Opt. Express **27**(6), 8912 (2019).
13. P. Chvojka, Z. Ghassemlooy, F. Cacialli, I. Darwazeh, S. Zvanovec, P. A. Haigh, A. Minotto, A. Burton, P. Murto, Z. Genene, W. Mammo, M. R. Andersson, and E. Wang, "Expanded Multiband Super-Nyquist CAP Modulation for Highly Bandlimited Organic Visible Light Communications," *IEEE Syst. J.* 1–7 (2019).
14. P. Chvojka, S. Zvanovec, K. Werfli, P. A. Haigh, and Z. Ghassemlooy, "Variable m-CAP for Bandlimited Visible Light Communications," in *2017 IEEE Int. Conf. Commun. Work. ICC Work. 2017*, (2017), pp. 1–5.
15. J. Wei and E. Giacoumidis, "Multi-band CAP for Next-Generation Optical Access Networks Using 10-G Optics," J. Lightwave Technol. **36**(2), 551–559 (2018).
16. Y. Wang, L. Tao, X. Huang, J. Shi, and N. Chi, "8-Gb/s RGBY LED-Based WDM VLC System Employing High-Order CAP Modulation and Hybrid Post Equalizer," IEEE Photonics J. **7**(6), 1–7 (2015).
17. J. A. Altabas, S. Rommel, R. Puerta, D. Izquierdo, J. I. Garces, J. A. Lazaro, J. J. V. Olmos, and I. T. Monroy, "Nonorthogonal Multiple Access and Carrierless Amplitude Phase Modulation for Flexible Multiuser Provisioning in 5G Mobile Networks," J. Lightwave Technol. **35**(24), 5456–5463 (2017).
18. S. Ahmadi, "Downlink Physical Layer Functions," in *LTE-Advanced*, (2014), pp. 399–720.
19. J. Dang and Z. Zhang, "Comparison of Optical OFDM-IDMA and Optical OFDMA for Uplink Visible Light Communications," in *2012 Int. Conf. Wirel. Commun. Signal Process.*, (2012), pp. 1–6.
20. C. Chen, D. Tsonev, and H. Haas, "Joint Transmission in Indoor Visible Light Communication Downlink Cellular Networks," in *2013 IEEE Globecom Work. (GC Wkshps)*, (2013), pp. 1127–1132.

Optics EXPRESS

21. C. Chen, S. Videv, D. Tsonev, and H. Haas, "Fractional Frequency Reuse in DCO-OFDM-Based Optical Attocell Networks," J. Lightwave Technol. **33**(19), 3986–4000 (2015).
22. J. Fakidis, D. Tsonev, and H. Haas, "A Comparison between DCO-OFDMA and Synchronous One-Dimensional OCDMA for Optical Wireless Communications," in *IEEE Int. Symp. Pers. Indoor Mob. Radio Commun. PIMRC*, (2013), pp. 3605–3609.
23. M. M. Merah, H. Guan, and L. Chassagne, "Experimental Multi-User Visible Light Communication Attocell Using Multiband Carrierless Amplitude and Phase Modulation," IEEE Access **7**, 12742–12754 (2019).
24. Y. Wang, L. Tao, Y. Wang, and N. Chi, "High Speed WDM VLC System Based on Multi-Band CAP64 with Weighted Pre-Equalization and Modified CMMA Based Post-Equalization," IEEE Commun. Lett. **18**(10), 1719–1722 (2014).
25. J. Zhang, J. Yu, F. Li, N. Chi, Z. Dong, and X. Li, "11 × 5 × 9.3Gb/s WDM-CAP-PON Based on Optical Single-Side Band Multi-Level Multi-Band Carrier-Less Amplitude and Phase Modulation with Direct Detection," Opt. Express **21**(16), 18842–18848 (2013).
26. J. L. Wei, C. Sanchez, and E. Giacoumidis, "Fair Comparison of Complexity Between a Multi-Band CAP and DMT for Data Center Interconnects," Opt. Lett. **42**(19), 3860 (2017).
27. C. Chen, M. Ijaz, D. Tsonev, and H. Haas, "Analysis of Downlink Transmission in DCO-OFDM-based Optical Attocell Networks," in *2014 IEEE Glob. Commun. Conf. GLOBECOM 2014*, (2014), pp. 2072–2077.
28. L. Feng, R. Q. Hu, J. Wang, P. Xu, and Y. Qian, "Applying VLC in 5G networks: Architectures and Key Technologies," IEEE Netw. **30**(6), 77–83 (2016).
29. Y. Chen, A. Lobato, Y. Jung, H. Chen, V. A. J. M. Sleiffer, M. Kuschnerov, N. K. Fontaine, R. Ryf, D. J. Richardson, B. Lankl, and N. Hanik, "41.6 Tbit/s C-band SDM OFDM Transmission through 12 Spatial and Polarization Modes over 74.17 km Few Mode Fiber," J. Lightwave Technol. **33**(7), 1440–1444 (2015).
30. K. O. Akande and W. O. Popoola, "Impact of Timing Jitter on the Performance of Carrier Amplitude and Phase Modulation," in *2016 Int. Conf. Students Appl. Eng. ICSAE 2016*, (2017), pp. 259–263.
31. M. A. Khalighi, S. Long, S. Bourennane, and Z. Ghassemlooy, "PAM-A and CAP-Based Transmission Schemes for Visible-Light Communications," IEEE Access **5**, 27002–27013 (2017).